MONITORING DELAMINATION OF THERMAL BARRIER COATINGS DURING INTERRUPED HIGH-HEAT-FLUX LASER TESTING USING UPCONVERSION LUMINESCENCE IMAGING

Jeffrey I. Eldridge and Dongming Zhu
NASA Glenn Research Center
Cleveland, OH 44135

Douglas E. Wolfe
Applied Research Laboratory
The Pennsylvania State University
University Park, PA 16802

ABSTRACT

Upconversion luminescence imaging of thermal barrier coatings (TBCs) has been shown to successfully monitor TBC delamination progression during interrupted furnace cycling. However, furnace cycling does not adequately model engine conditions where TBC-coated components are subjected to significant heat fluxes that produce through-thickness temperature gradients that may alter both the rate and path of delamination progression. Therefore, new measurements are presented based on luminescence imaging of TBC-coated specimens subjected to interrupted high-heat-flux laser cycling exposures that much better simulate the thermal gradients present in engine conditions. The TBCs tested were deposited by electron-beam physical vapor deposition (EB-PVD) and were composed of 7wt% yttria-stabilized zirconia (7YSZ) with an integrated delamination sensing layer composed of 7YSZ co-doped with erbium and ytterbium (7YSZ:Er,Yb). The high-heat-flux exposures that produce the desired through-thickness thermal gradients were performed using a high power CO_2 laser operating at a wavelength of 10.6 microns. Upconversion luminescence images revealed the debond progression produced by the cyclic high-heat-flux exposures and these results were compared to that observed for furnace cycling.

INTRODUCTION

The demonstration of nondestructive diagnostic tools for monitoring delamination progression for TBC-coated specimens due to thermal cycling has been mostly limited to exposure to furnace environments, where thermal cycling alternates between hot and cold isothermal conditions. However, furnace cycling does not adequately simulate turbine engine conditions, where TBC-coated components are subjected to significant heat fluxes that are not present in a furnace environment. These heat fluxes produce through-thickness temperature gradients that may alter both the rate and pathway of TBC delamination progression. In contrast to the non-evolving temperature profiles associated with furnace cycling, temperature gradients through TBCs subjected to high heat fluxes will also change over the course of cycling due to TBC sintering and the generation of delamination cracks, both of which will affect heat transport through the TBC. Therefore, diagnostics developed to predict remaining TBC life in engine environments must be based on testing of TBCs subjected to engine-like heat flux conditions.

Luminescence imaging of TBCs incorporating an integrated delamination sensing layer has been shown to provide exceptionally high contrast for monitoring TBC delamination.[1,2] The

objective of this paper is to extend luminescence-based delamination monitoring to TBCs subjected to high heat flux. To meet this objective, upconversion luminescence imaging has been applied to monitor TBC delamination progression in TBC-coated specimens subjected to high heat fluxes produced by a high-power CO_2 laser. The delamination progression revealed by upconversion luminescence imaging for two different heat fluxes is compared with the delamination progression produced by furnace cycling.

EXPERIMENTAL PROCEDURES
Upconversion Luminescence Imaging
  Upconversion luminescence refers to the special case of luminescence where the emission wavelength, λ_{em}, is shorter (higher energy) than the excitation wavelength, λ_{ex}. Upconversion luminescence is attractive for delamination monitoring because of the absence of background emission at wavelengths shorter than the excitation wavelength, resulting in superior contrast. Fig. 1 shows the concept and the coating design behind monitoring TBC delamination by upconversion luminescence imaging. The 7YSZ TBC incorporates a thin base layer that is co-doped with erbium and ytterbium (YSZ:Er,Yb) below a thicker undoped YSZ layer. Erbium was selected as a dopant specifically because a two-photon excitation ($\lambda_{ex} = 980$ nm) from the $^4I_{15/2}$ ground state of Er^{3+} to the $^4F_{7/2}$ excited state can produce upconversion luminescence emission at $\lambda_{em} = 562$ nm, corresponding to the relaxation from the $^4S_{3/2}$ excited state back to the $^4I_{15/2}$ ground state of Er^{3+}.[4] The Yb^{3+} co-dopant is added because Yb^{3+} is a better absorber of the 980 nm excitation (via excitation from the Yb^{3+} $^2F_{7/2}$ ground state to the $^2F_{5/2}$ excited state) than Er^{3+} and can then transfer the excitation energy to Er^{3+} to produce luminescence. The delamination contrast that is desired is achieved because when delamination cracks form near the bottom of the TBC, these cracks introduce interfaces that are highly reflective for both the excitation and emission wavelengths so that significantly higher luminescence intensity is observed from regions containing delamination cracks.[1,2]
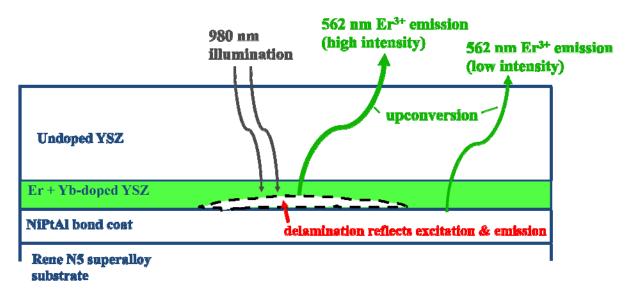

Figure 1. Concept for monitoring TBC delamination progression by upconversion luminescence.

The excitation source for the upconversion luminescence was a 980 nm laser diode that illuminated the specimen after the laser beam traveled through beam expanding optics. The upconversions luminescence images were collected by a cooled CCD camera with a bandpass filter centered at 562 nm (FWHM = 40 nm) and an image acquisition time of 3.25 sec. A background subtraction was performed for each upconversion luminescence image followed by normalization to an unconversion luminescence image of an uncycled control specimen.
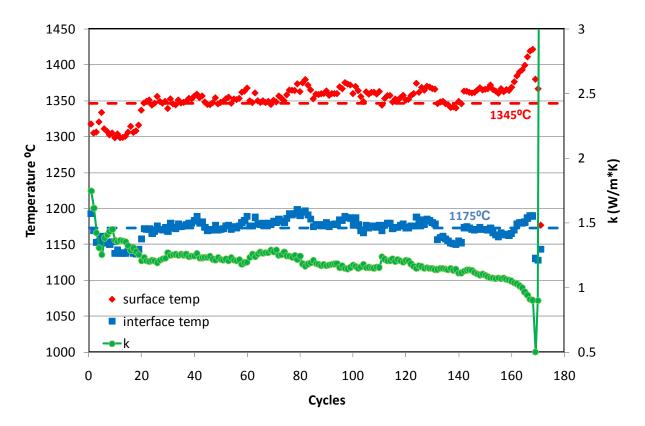
Specimens
TBCs were deposited by multiple ingot electron-beam physical vapor deposition (EB-PVD) at Penn State and consisted of an initial 11 µm Er+Yb co-doped YSZ layer (cation dopant mole concentrations of 1% Er and 3% Yb) followed by a 135 µm thick undoped 7YSZ overlayer which was deposited with no disruption of the columnar growth between layers in a manner previously described.[1-3] The TBCs were deposited onto NiPtAl bond-coated (Chromalloy) nickel-based superalloy Rene N5 substrates (25.4 mm diameter, 3.18 mm thick).

High-Heat-Flux Laser Testing
TBC-coated specimens were subjected to heat fluxes using the NASA GRC high-heat-flux laser facility.[5] In short, a combination of high power CO_2 laser (wavelength = 10.6 µm) heating of the surface of the TBC combined with forced air backside cooling produced the desired heat flux. The heat flux through the specimen was determined by subtracting heat flux losses by reflection and radiation from the heat flux delivered by the laser. TBC surface temperatures were determined by an 8 µm pyrometer and the substrate backside temperatures by a two-color pyrometer. As previously shown,[5] the apparent thermal conductivity of the TBC, k_{TBC}, could be determined from the heat flux, top and backside temperatures, and known substrate thermal conductivity. For the laser cyclic testing, one cycle consisted of 60 min with the laser on followed by 3 min with the laser off.
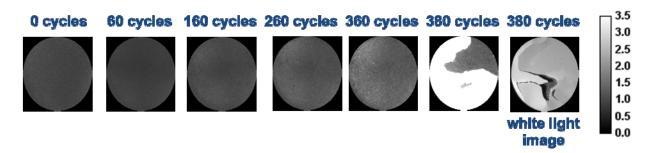
Two heat flux conditions were examined. A lower heat flux of 95 W/cm^2 produced nominal surface and TBC/bond coat interface temperatures of 1290⁰C and 1140⁰C, respectively, while a higher heat flux of 125 W/cm^2 produced nominal surface and interface temperatures of 1345⁰C and 1175⁰C, respectively. As shown in Fig. 2 for the higher heat flux test, actual temperatures fluctuated somewhat from these nominal temperatures, and there was a drift upward in the TBC surface temperature, especially toward the end of cyclic life. Upconversion luminescence images were collected during interruptions in laser cycling (typically after 20 cycle intervals). Results from the laser testing were compared with conventional furnace cycling in a tube furnace where each cycle consisted of 45 min at 1163⁰C followed by 15 min cooling (to ~120⁰C) and upconversion luminescence images were collected at interruptions in furnace cycling (also typically after 20 cycle intervals). All laser and furnace cycle testing was performed on specimens with TBCs deposited in the same EB-PVD run. One specimen was cycled to failure at each of the heat flux conditions and two specimens were cycled to failure by furnace cycling.
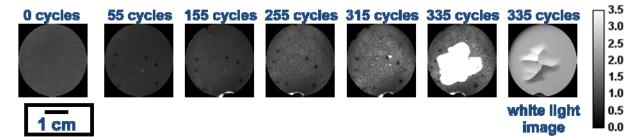
Figure 2. TBC surface (red diamond), interface (blue square) temperatures and apparent k_{TBC} (green circles) as a function of laser cycles for the 125 W/cm^2 heat flux testing.
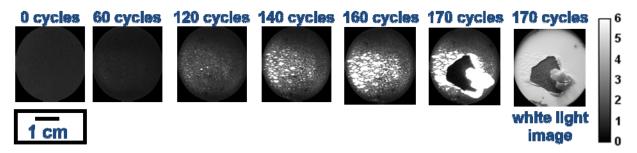
RESULTS

A selected subset of the upconversion luminescence images collected during furnace cycling and for interrupted laser cycle testing at 95 and 125 W/cm^2 heat flux conditions in Figs. 3, 4, and 5, respectively.

Figure 3. Upconversion luminescence images collected during interrupted furnace cycling to 1163°C along with white light image of final specimen failure at 380 funace cycles. Normalized intensity scale indicates ratio of intensity to that of an uncycled control specimen.

Figure 4. Upconversion luminescence images collected during interrupted laser cycling with heat flux of 95 W/cm^2 along with white light image of final specimen failure at 335 cycles. Normalized intensity scale indicates ratio of intensity to that of an uncycled control specimen.
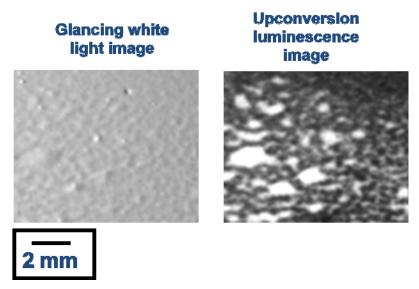

Figure 5. Upconversion luminescence images collected during interrupted laser cycling with heat flux of 125 W/cm^2 along with white light image of final specimen failure at 170 cycles. Normalized intensity scale indicates ratio of intensity to that of an uncycled control specimen.
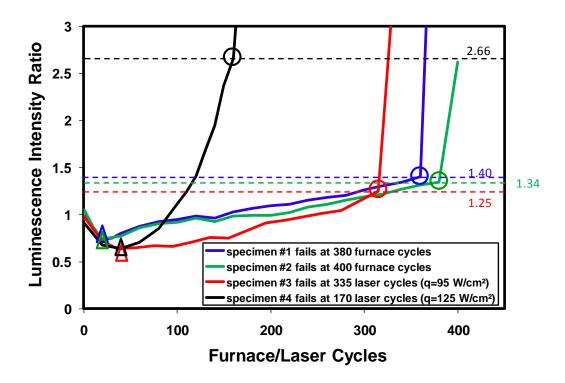
In all cases, an initial reduction in luminescence intensity is observed followed by a gradual, but consistent increase in luminescence intensity that is spotty in nature, although the increase in luminescence is less spotty for the furnace cycling test. Cycling was continued until macroscopic failure was observed (see white light images in Figs. 3, 4, and 5), consisting of TBC buckling after 380 furnace cycles, TBC buckling for the 95 W/cm^2 heat flux after 335 laser cycles, and TBC spallation for the 125 W/cm^2 heat flux after 170 laser cycles. Note that the bright spots in the luminescence images, corresponding to local TBC/substrate separations, cover a much higher fraction of the image area prior to macroscopic failure for the higher 125W/cm^2 heat flux.

While the lower heat flux (95 W/cm^2) cycling and the furnace cycling showed no evidence of delamination progression to the naked eye until final TBC macroscopic failure, this was not the case for the higher heat flux (125 W/cm^2) cycling where undulations of the TBC surface were evident under glancing illumination well before final macroscopic TBC failure (Fig. 6). It is clear that the raised areas of the TBC surface correspond to the bright areas in the upconversion luminescence image, indicating that the raised areas correspond to regions where there is a local TBC/substrate separation. This surface texturing has been observed previously,[6,7] and has been attributed to bond coat rumpling beneath the TBC.

Glancing white light image

Upconversion luminescence image

2 mm

Figure 6. Higher magnification images of region of TBC-coated specimens after 155 laser cycles with heat flux of 125 W/cm^2. (Left) White light image under glancing illumination. (Right) Upconversion luminescence image of same area.

The changes in upconversion luminescence intensity can be compared more quantitatively by plotting the normalized luminescence intensity averages over the entire area of each specimen image as a function of cycles as shown in Fig. 7 for the 95 and 125 W/cm^2 heat flux laser cycling tests as well as the two 1163°C furnace cycling tests. All the plots show several features in common: (1) an initial decrease in luminescence intensity until minimum is reach (marked by triangles in Fig. 7) followed by (2) a gradual increase in intensity associated with debond progression and (3) a substantial inflection upward (marked by circles in Fig. 7) associated with macroscopic TBC failure. In addition, both furnace cycling tests and the 95 W/cm^2 heat flux laser cycling test exhibited the onset of macroscopic TBC failure (marked by circles in Fig. 7) at about the same normalized luminescence intensity. Significant differences included the 95 W/cm^2 laser cycling test exhibiting an initial incubation period where significant luminescence increase was not observed until beyond 100 cycles, followed by an accelerating increase in luminescence intensity. The behavior for the 125 W/cm^2 laser cycling test exhibited pronounced differences in comparison to the lower heat flux laser cycling or furnace cycling: not only was the rate of luminescence increase faster (not unexpected in view of the higher interface temperatures), but the average normalized luminescence increased to much higher intensity before the onset of macroscopic TBC failure.

Figure 7. Normalized upconversion luminescence intensity averages over entire specimen image as a function of cycles. Comparison in behavior for furnace cycling (at 1163⁰C), and two conditions of high-heat-flux laser cycling ($q = 95$ and 125 W/cm^2). Circles mark first observation of macroscopic TBC failure. Triangles mark minimum luminescence.

DISCUSSION

Upconversion luminescence imaging was used to compare TBC delamination progression due to thermal cycling under two laser-induced heat flux conditions with delamination progression produced by furnace cycling. In all cases, an initial reduction in upconversion luminescence intensity was observed (Fig. 7) that is most likely associated with growth of the thermally grown oxide (TGO) beneath the TBC resulting in a less reflective substrate. The bright spots in the luminescence images (Figs. 3-6) are associated with local delamination cracks that act as highly reflective interfaces for both the $\lambda_{ex} = 980$ nm excitation and $\lambda_{ex} = 562$ nm upconversion emission. The growth in number, size, and intensity of these bright spots is proposed to correspond to the generation, lateral growth, and increasing crack opening, respectively, of delamination cracks. Preliminary SEM inspection of previously furnace cycled TBC-coated specimens has verified the presence of isolated local delaminations. SEM investigation of the cross-sections of the laser and furnace cycled TBC-coated specimens tested for this paper have not yet been performed but are planned.

While the general trend of debond progression by generation of delamination cracks that grow in number and extent and coalesce until macroscopic TBC failure is observed in all cases

(Figs. 3-6), significant differences were also observed. Some of the observed differences may be attributed to differences in the interface temperatures during cycling, which were 1140⁰C and 1175⁰C for the 95 W/cm^2 and 125 W/cm^2 heat flux laser cycling, respectively, and an intermediate 1163⁰C for the furnace cycling tests. Some differences could also be due to the shorter hot cycle duration (45 min vs. 60 min) for the furnace cycle tests, and the faster heating and cooling associated with the laser cycling tests. To determine the effects of heat flux on delamination progression, furnace cycling should be performed at temperatures that match the interface temperatures during the heat flux laser tests (furnace cycling at 1140⁰C and 1175⁰C) and with the same hot time duration (60 min), and this is planned for future work. However, the present results still suggest effects of heat flux on delamination progression as described below.

While the onset of macroscopic failure intensity occurred at about the same normalized luminescence intensity for the lower 95 W/cm^2 heat flux laser cycling and the furnace cycling tests (Fig. 7), the 95 W/cm^2 laser cycling exhibits an incubation period until about 100 laser cycles before the increases in luminescence intensity associated with delamination progression are observed. This incubation (or latent) period is followed by an accelerating increase in luminescence intensity in comparison to the furnace cycling tests. Although only one laser cycling test was performed at this heat flux, this behavior was very out-of-character in comparison to the furnace cycling tests, where this behavior was not observed not only from the 2 furnace cycling tests from the same TBC deposition batch (Fig. 7), but also never observed in furnace cycling under the same conditions for 16 other specimens from other TBC deposition batches. These results suggest that the 95 W/cm^2 heat flux does not accelerate delamination initiation. However, it is proposed that once delamination cracks are established, the heat flux significantly accelerates delamination progression. It is important, therefore, to realize that the equivalent interface damage accumulation appears to occur much later in the laser cycling than in the furnace cycling (damage accumulation proceeds more uniformly during furnace cycling, but is weighted more heavily towards the end of life during laser cycling). Therefore, a prediction of TBC remaining based on interface damage accumulation during furnace cycling would grossly overestimate remaining life when heat flux effects are present.

The higher 125 W/cm^2 laser cycling test does not exhibit the same prolonged incubation period as the lower 95 W/cm^2 test; however, onset of delamination progression (luminescence intensity increase marked by black triangle in Fig. 7) is still delayed in comparison with the furnace cycling tests despite the higher interface temperature attained in the 125 W/cm^2 laser cycling (1175⁰ C vs. 1163⁰C). This comparison suggests that the high heat flux may actually suppress delamination initiation. However, following delamination initiation, the rate of luminescence increase (delamination damage accumulation) is greatly accelerated for the higher heat flux laser cycling test. Perhaps the most striking difference observed for the higher heat flux laser cycling test is that the delamination damage associated with bright luminescence (Figs. 5-7) accumulates to a much greater extent before macroscopic TBC failure occurs, suggesting that under the conditions of higher heat flux and higher interface and surface temperatures, the TBC can accommodate a much higher degree of damage before producing macroscopic TBC buckling or spallation. This very different behavior may be related to a different mechanism driving delamination progression. In particular, TBC surface undulations (Fig. 6) associated with bond coat rumpling beneath the TBC were only observed for the higher heat flux condition. The luminescence images clearly indicate that the raised portions of the TBC surface (corresponding to peaks in the surface of the rumpled bond coat below) are associated with local areas of TBC/substrate separation; therefore, delamination progression in the higher heat flux testing

appears to be driven by bond coat rumpling. The much greater role of bond coat rumpling in the delamination progression in the higher heat flux test may be partly due to the higher interface temperature that will promote bond coat rumpling because of higher rates of diffusion in the bond coat, but may also be due to the heat flux contribution which results in higher TBC temperatures above the interface that will reduce the stiffness of the TBC (along with higher TBC creep rates) and therefore reduce the constraint to bond coat rumpling that the TBC provides.[6,7] Because bond coat rumpling allows a local lengthening of the TGO, rumpling will therefore significantly reduce strain energy near the interface so that the stress intensity at a crack tip along the rumpled bond coat surface will be significantly less than in the absence of bond coat rumpling. This rumpling-induced reduction of crack tip stress intensity will make local TBC buckling more stable against further growth and therefore explain the accommodation of greater delamination damage accumulation prior to macroscopic failure when bond coat rumpling occurs.

TBC delamination produced by thermal cycling has been shown to be driven by TGO growth, mismatch strain energy produced during cooling cycles,[8,9] along with effects of bond coat rumpling[6,7] and effects of TBC sintering.[10] These delamination driving forces can all be affected by heat flux effects as described below.

While TGO growth should only be dependent on interface temperature irrespective of heat flux, delamination cracks can lead to increased temperature at delamination crack tips. For a sufficient crack opening, a delamination crack in the presence of a heat flux will experience a temperature difference, ΔT_{crack}, across the crack, and therefore the temperature above the crack will be greater than at regions away from the crack. Therefore, the temperature at the crack tip will be intermediate between the temperature just above the crack and the temperature at a lateral distance away from the crack, the crack tip temperature will be higher than at distances away from the crack and therefore produce faster TGO growth at the crack tip.

In addition to stresses produced by TGO growth, Evans and Hutchinson[9] have shown that the steady state linear elastic energy release rate for delamination at the TBC/substrate interface during cooling, including release of forces and moments induced by heat fluxes, is

$$G = \frac{d(1-\upsilon_{TBC}^2)}{6E_{TBC}}(3\bar{\sigma}^2 + \sigma_0^2) \tag{1}$$

where d is the TBC thickness, and E_{TBC} and ν_{TBC} are the elastic modulus and the Poisson's ratio of the TBC, respectively, and σ_0 and $\bar{\sigma}$ are given by

$$\sigma_0 = \frac{E_{TBC}\alpha_{TBC}\Delta T_{surf/int}}{2(1-\upsilon_{TBC})} \tag{2}$$

$$\bar{\sigma} = \frac{E_{TBC}}{1-\upsilon_{TBC}}\left[\frac{\Delta T_{surf/int}}{2} - \Delta\alpha\Delta T_{int}\right] \tag{3}$$

where ΔT_{int} is the temperature drop of the interface from its peak temperature, $\Delta T_{surf/int}$ is the temperature drop of the surface minus the temperature drop of the interface, α_{TBC} is the coefficient of thermal expansion of the TBC and $\Delta\alpha$ is the coefficient of thermal expansion of the substrate minus that of the TBC. Essentially, $\bar{\sigma}$ is the average stress in the TBC and σ_0 is the difference in stress between the TBC surface and interface upon cooling. Note that σ_0 is purely a heat flux effect and is zero in the absence of a heat flux where $\Delta T_{surf/int} = 0$. On the other hand, the heat flux contribution in equation 2 (first term) acts in opposition to the TBC/substrate mismatch strain and therefore will reduce $\bar{\sigma}$. A priori, it is not known whether the introduction

of a heat flux will increase G (equation 1), since that will depend on whether the increase in σ_0 more than offsets the increase in $\bar{\sigma}$. Because the observed effect of a heat flux (Fig. 7) seems to be to modestly delay debond initiation compared to furnace cycling, the results suggest that the heat flux reduces G at the initial stages of crack propagation.

High heat fluxes can also produce sintering at the higher temperatures near the TBC surface and therefore increase k_{TBC} and produce a thermal conductivity gradient across the TBC thickness with highest thermal conductivity at the surface.[10] Note that the *decrease* in apparent k_{TBC} observed in Fig. 2 is due to the effect of delamination cracks producing a barrier to heat transport. The resulting thermal conductivity gradient will produce an associated change in the thermal profile across the TBC. In addition, sintering will result in an increased effective modulus of the TBC, thereby increasing both $\bar{\sigma}$ and σ_0 and therefore G. The effect of the dimensional sintering-induced shrinkage is less unequivocal since this shrinkage will increase σ_0 but decrease $\bar{\sigma}$.

Finally, the effect of heat flux will also be to reduce the effective TBC stiffness at high temperature due to the higher TBC temperatures above the interface (resulting in lower modulus and higher creep rates). This reduced stiffness will lessen the degree to which the TBC constrains bond coat rumpling, therefore promoting bond coat rumpling induced delamination. Bond coat rumpling will accelerate delamination crack accumulation, but will also accommodate a greater damage accumulation before triggering macroscopic TBC failure because of the strain relaxation that accompanies rumpling.

SUMMARY

Upconversion luminescence imaging successfully monitored TBC delamination progression for both interrupted furnace cycling and high-heat-flux laser cycling tests. It appears that the effect of heat flux is to first delay initial TBC delamination progression due to slightly reduced thermal expansion mismatch stresses, but to then greatly accelerate delamination progression after delamination progression is established, presumably due to an evolution of the mechanical properties of the TBC along with associated changes in the thermal profile across its thickness. Heat fluxes can also promote bond coat rumpling by reducing the TBC stiffness constraint against rumpling, thereby changing the character of the delamination progression. It is proposed that rumpling-induced local delamination produces more stress relief than local delamination produced without bond coat rumpling so that rumpling-induced local delaminations are more resistant to crack growth. Finally, life prediction based on observed damage evolution occurring during furnace cycling will grossly overestimate TBC remaining life under high heat flux conditions.

ACKNOWLEDGMENTS

REFERENCES

[1]J.I. Eldridge, T.J. Bencic, C.M. Spuckler, J. Singh, and D.E. Wolfe, "Delamination-Indicating Thermal Barrier Coatings Using YSZ:Eu Sublayers," *J. Am.. Ceram. Soc.*, **89**[10], 3246-3251 (2006).

[2]J.I. Eldridge and T.J. Bencic, "Monitoring Delamination of Plasma-Sprayed Thermal Barrier Coatings by Reflectance-Enhanced Luminescence," *Surf. Coat. Technol*., **201**[7], 3926-3930 (2006).

[3]J.I. Eldridge, J. Singh, and D.E. Wolfe, "Erosion-Indicating Thermal Barrier Coatings Using Luminescent Sublayers, *J. Amer. Ceram. Soc.*, **89**[10], 3252-3254 (2006).

[4] H. Berthou and C.K. Jörgensen, "Optical-Fiber Temperature Sensor Based on Upconversion-Excited Fluorescence," *Optics Lett.*, **15**[19], 1100-1102 (1990).

[5]D. Zhu, R.A. Miller, B.A. Nagaraj, and R.W. Bruce, "Thermal Conductivity of EB-PVD Thermal Barrier Coatings Evaluated by a Steady-State Laser Heat Flux Technique," *Surf. Coat. Technol.*, **138**[1], 1-8 (2001).

[6]V.K. Tolpygo and D.R. Clarke, "Morphological Evolution of Thermal Barrier Coatings Induced by Cyclic Oxidation," *Surf. Coat. Technol.*, **163-164**, 81-86 (2003).

[7]V.K. Tolpygo, D.R. Clarke, and K.S. Murphy, "Evolution of Interface Degradation During Cyclic Oxidation of EB-PVD Thermal Barrier Coatings and Correlation with TGO Luminescence," *Surf. Coat. Technol.*, **188-189**, 62-70 (2004).

[8]J.W. Hutchinson and A.G. Evans, "On the Delamination of Thermal Barrier Coatings in a Thermal Gradient," *Surf. Coat. Technol*., **149**, 179-184 (2002).

[9]A.G. Evans and J.W. Hutchinson, "The Mechanics of Coating Delamination in Thermal Gradients," *Surf. Coat. Technol.*, **201**, 7905-7916 (2007).

[10]Y. Tan, J.P. Longtin, S. Sampath, and D. Zhu, "Temperature-Gradient Effects in Thermal Barrier Coatings: An Investigation Through Modeling, High Heat Flux Test, and Embedded Sensor," *J. Am. Ceram. Soc.*, **93**[10], 3418-3426 (2010).